Published in final edited form as:
*Nat Genet*. ; 43(7): 639–647. doi:10.1038/ng.860.

# A genetic interaction network of five genes for human polycystic kidney and liver diseases defines polycystin-1 as the central determinant of cyst formation

**Sorin V Fedeles**[1,2], **Xin Tian**[1,6], **Anna-Rachel Gallagher**[1,6], **Michihiro Mitobe**[1], **Saori Nishio**[1], **Seung Hun Lee**[1], **Yiqiang Cai**[1], **Lin Geng**[1], **Craig M Crews**[3,5], and **Stefan Somlo**[1,2]

[1]Department of Internal Medicine, Yale University School of Medicine, New Haven, Connecticut, USA

[2]Department of Genetics, Yale University School of Medicine, New Haven, Connecticut, USA

[3]Department of Molecular, Cellular and Developmental Biology, Yale University School of Medicine, New Haven, Connecticut, USA

[4]Department of Pharmacology, Yale University School of Medicine, New Haven, Connecticut, USA

[5]Department of Chemistry, Yale University School of Medicine, New Haven, Connecticut, USA

## Abstract

Autosomal dominant polycystic liver disease results from mutations in *PRKCSH* or *SEC63*. The respective gene products, glucosidase IIβ and SEC63p, function in protein translocation and quality control pathways in the endoplasmic reticulum. Here we show that glucosidase IIα and Sec63p are required in mice for adequate expression of a functional complex of the polycystic kidney disease gene products, polycystin-1 and polycystin-2. We find that polycystin-1 is the rate-limiting component of this complex and that there is a dose-response relationship between cystic dilation and levels of functional polycystin-1 following mutation of *Prkcsh* or *Sec63*. Reduced expression of polycystin-1 also serves to sensitize the kidney to cyst formation resulting from mutations in *Pkhd1*, the recessive polycystic kidney disease gene. Finally, we show that proteasome inhibition increases steady-state levels of polycystin-1 in cells lacking glucosidase IIβ and that treatment with a proteasome inhibitor reduces cystic disease in orthologous gene models of human autosomal dominant polycystic liver disease.

Polycystic liver disease (PLD) is an inherited condition characterized by the presence of multiple scattered cysts of biliary origin throughout the liver parenchyma[1]. PLD occurs frequently as an extra-renal manifestation of autosomal dominant polycystic kidney disease (ADPKD; MIM173900 and MIM173910), but it also exists as a distinct dominantly



Correspondence should be addressed to S.S. (stefan.somlo@yale.edu). .
[6]These authors contributed equally to this work.

Note: Supplementary information is available on the Nature Genetics website.

**AUTHOR CONTRIBUTIONS** S.V.F. co-designed the study, performed the experiments and co-wrote the manuscript. X.T. and M.M. generated the mouse models. A.-R.G. performed experiments, participated in the experimental design and assisted in manuscript preparation. S.N., S.H.L., Y.C. and L.G. carried out experiments. C.M.C. participated in the proteasome inhibitor studies. S.S. came up with the study design and co-wrote the manuscript.

**COMPETING FINANCIAL INTERESTS** The authors declare no competing financial interests.

inherited genetic entity without kidney cysts (ADPLD; MIM174050). Mutations in *PRKCSH* or *SEC63* underlie isolated ADPLD[2–5]. The *SEC63* gene product, SEC63p, works in concert with the SEC61 translocon and BiP to facilitate co-translational translocation across the endoplasmic reticulum (ER) membrane of nascent peptides destined to become either secreted or membrane-inserted proteins[6–8]. *PRKCSH* encodes the non-catalytic β-subunit of glucosidase II (GIIβ)[9,10]. Glucosidase II activity is necessary for proper folding and quality control of proteins passing through the ER translocon[11]. The ADPLD-associated GIIβ subunit contains an ER luminal retention signal and is required for function of the glucosidase II holoenzyme[12]. The two causative genes for ADPKD, *PKD1* and *PKD2*, encode polycystin-1 (PC1) and polycystin-2 (PC2), respectively[13–15]. PC1 and PC2 are integral membrane proteins thought to function as a $Ca^{2+}$-permeable receptor-channel complex in the cilia membrane[16–18]. The causative gene for autosomal recessive polycystic kidney disease (ARPKD; MIM263200), *PKHD1*, encodes fibrocystin/polyductin (FPC), another complex integral membrane protein localized to cilia as well as other cellular compartments[19–21].

PC1, PC2 and FPC, along with one Meckel syndrome gene product (MKS3)[22], are the only integral membrane proteins mutated in cilia-associated fibrocystic diseases[23]. PC1 and FPC are particularly large proteins (>4,000 amino acids) predicted to have extensive post-translational modifications, including proteolytic processing[24,25]. ADPKD and ADPLD are also unique in that they are the only dominantly inherited traits among the cilia-associated diseases[26]. At the cellular level, kidney and liver cysts in ADPKD occur by a recessive mechanism resulting from somatic second-step mutations[27–29]. The timing of second hits affects the rate of cyst growth, with perinatal inactivation resulting in more rapid growth; however, adult inactivation of polycystins is sufficient to produce ADPKD[30,31]. Clinically, liver cysts in ADPLD are indistinguishable from those found in ADPKD[1,32], yet GIIβ and SEC63p are the two clearest examples of gene products associated with polycystic disease but not with the cilia-basal–body complex[4]. To understand the mechanisms underlying ADPLD and the role of non-ciliary proteins in polycystic diseases, we used mouse mutants to analyze the genetic and functional interrelationship of *Prkcsh* and *Sec63* with the three major polycystic disease genes encoding membrane-inserted glycoproteins (*Pkd1*, *Pkd2* and *Pkhd1*). We show that tissue-selective homozygous loss-of-function mutations in *Prkcsh* or *Sec63* result in cyst formation in the kidney as well as in the liver. We further show that loss of either GIIβ or Sec63p results in reduced levels of functional PC1-PC2 complex, with PC1 acting as the rate-limiting component determining the severity of the cystic phenotype. In addition, we show that expression levels of PC1 can modify the severity of kidney cyst formation caused by mutations in *Pkhd1*. Finally, we show that inhibition of proteasome activity increases the steady-state levels of PC1 in cells lacking GIIβ, and that treatment with a protea-some inhibitor improves cystic disease in orthologous gene models of human ADPLD.

## RESULTS

### Loss of *Prkcsh* and *Sec63* leads to kidney and liver cysts

We began by establishing *in vivo* models of ADPLD based on conditional alleles for *Prkcsh* and *Sec63* in mice (Figs. 1 and 2). Deletion of the conditional alleles resulted in a complete loss of expression of the respective proteins in kidney epithelial cell lines from $Prkcsh^{flox/flox}$ and $Sec63^{flox/flox}$ mice (Fig. 1a, left panels). The liver and kidney phenotypes of homozygous null $Prkcsh^{-/-}$ and $Sec63^{-/-}$ mice could not be evaluated because of early embryonic lethality (Supplementary Note), so we used tissue selective and inducible expression of Cre for the *in vivo* studies (Fig. 1a, right panels). Induction of gene inactivation in adult $Prkcsh^{flox/flox}$; *pCX-CreER* mice (Fig. 1b) and $Sec63^{flox/flox}$; *pCX-CreER* mice (X.T., M.M., S.N. & S.S., data not shown) resulted in liver cyst formation,

establishing these mice as orthologous gene models for human ADPLD and showing the causal relationship between somatic second-step mutations and the occurrence of liver cysts. We next sought to determine whether the similarities between ADPLD and ADPKD phenotypes in the liver[29,31] extend to the kidney. We achieved kidney-selective inactivation of *Prkcsh* and *Sec63* using the *Ksp-Cre* transgenic line that drives expression of Cre recombinase in thick ascending loops of Henle (TAL), the distal convoluted tubule and cortical and medullary collecting duct segments[33,34]. The resultant polycystic kidney disease (PKD) phenotype with the ADPLD genes (Figs. 1c and 2a) was similar but milder than that observed following inactivation of *Pkd1* or *Pkd2* (refs. 34,35). Whereas $Pkd1^{flox/flox}$; *Ksp-Cre* mice do not survive past postnatal day (P) 17 (ref. 34), $Sec63^{flox/flox}$; *Ksp-Cre* mice live past P60, and $Prkcsh^{flox/flox}$; *Ksp-Cre* mice live past 6 months (Supplementary Note). The occurrence of PKD following inactivation of *Prkcsh* and *Sec63* prompted us to investigate the genetic and biochemical interrelationship between the ADPLD genes and *Pkd1* and *Pkd2*.

## *Pkd1* dosage determines cyst progression in ADPLD

We hypothesized that the basis of cyst formation following inactivation of *Prkcsh* and *Sec63* was related to ADPKD through defective biogenesis and expression of PC1 and PC2. We tested this by reducing the dosage of polycystins using the $Pkd1^{+/-}$ or $Pkd2^{+/-}$ backgrounds in the *Prkcsh* and *Sec63* PKD models. The severity of cystic disease as a function of genotype was quantified using kidney weight to body weight ratio, fraction of the total area in kidney sections occupied by cysts (cystic index) and serum urea nitrogen (BUN). $Prkcsh^{flox/flox}$; *Ksp-Cre* and $Sec63^{flox/flox}$; *Ksp-Cre* mice compounded with either the $Pkd1^{+/-}$ or $Pkd2^{+/-}$ background showed increased severity of PKD by all three criteria (Figs. 1c,d and 2a,b). The variation between genotypes was significantly greater than the variation within genotypes (Supplementary Figs. 1 and 2). The structural cystic phenotype with $Pkd1^{+/-}$ was consistently more severe than with $Pkd2^{+/-}$ in both *Prkcsh* and *Sec63* models, suggesting a greater sensitivity to the dose of PC1 (Figs. 1c,d and 2a,b and Supplementary Figs. 1 and 2).

We next used BAC transgenic overexpression of *Pkd1* and *Pkd2* to evaluate whether dosage of either gene was the predominant determinant of cyst formation in *Prkcsh* and *Sec63* mutant mice on the wild-type background. The $Pkd1^{F/H}$-BAC transgenic line (Tg248) has three copies of the transgene and expresses PC1 modified with an $NH_2$-terminal triple-FLAG epitope tag and a C-terminal triple-hemagglutinin (HA) epitope tag (Fig. 1e; M.M., Y.C. & S.S., data not shown). $Pkd1^{F/H}$-BAC rescues embryonic lethal $Pkd1^{-/-}$ mice, which remain healthy without kidney cysts for at least 12 months. The *Pkd2*-BAC line expresses unmodified PC2 at about fourfold higher levels than non-transgenic controls (Fig. 1e)[36]. The $Pkd1^{F/H}$-BAC transgene rescued the cystic kidney phenotype in both $Prkcsh^{flox/flox}$; *Ksp-Cre* and $Prkcsh^{flox/flox}$; *Ksp-Cre;*$Pkd2^{+/-}$ mice, indicating that PKD resulting from loss of *Prkcsh* as well as the exacerbation of the phenotype resulting from $Pkd2^{+/-}$ was overcome by *Pkd1* overexpression (Fig. 1c,d and data not shown). $Pkd1^{F/H}$-BAC had no effect on cysts following complete loss of *Pkd2*, indicating that PC1 requires some functional PC2 to rescue PKD (Fig. 1f). In contrast to results in zebrafish models[37], the *Pkd2*-BAC transgene had no apparent effect on kidney cysts in $Prkcsh^{flox/flox}$; *Ksp-Cre*; $Pkd1^{+/-}$ (Fig. 1c,d) or $Prkcsh^{flox/flox}$; *Ksp-Cre* mice. The finding that PC2 is required for PC1 function independently of PC1 dosage is consistent with the existence of an active PC1-PC2 complex[38,39].

As ADPLD manifests with liver cysts in humans, we determined whether *Pkd1* gene dosage was also the central determinant in bile duct cyst formation. We examined $Prkcsh^{flox/flox}$; *pCX-Cre* mice with and without the $Pkd1^{F/H}$-BAC and *Pkd2*-BAC transgenes eight weeks after tamoxifen induction. We used only male mice to avoid confounding effects of sex in

the progression of ADPLD. *Pkd1*, but not *Pkd2*, overexpression completely abrogated the ADPLD liver cystic phenotype (Fig. 1b). We next determined whether the dependence on *Pkd1* dosage in ADPLD was applicable to the more severe phenotypes resulting from inactivation of *Sec63*. The *Pkd1*$^{F/H}$-BAC rescued the cystic phenotype in *Sec63*$^{flox/flox}$; *Ksp-Cre* mice, whereas the *Pkd2-BAC* did not (Fig. 2a,b). We further examined the interrelationship of *Prkcsh* and *Sec63* using doubly mutant *Prkcsh*$^{flox/flox}$; *Sec63*$^{flox/flox}$; *Ksp-Cre* mice (Fig. 2c). The severity of cyst formation was markedly increased by simultaneous inactivation of both ADPLD genes. Because the products of both genes act in a common biogenetic pathway and because the cystic phenotypes are determined by *Pkd1* dosage in both forms of the disease, this additive effect supports the hypothesis that severity of cyst formation in ADPLD is dynamically determined by PC1 levels.

## Impaired biogenesis of PC1 following loss of *Prkcsh* or *Sec63*

These genetic data, coupled with the known functions of GIIβ and Sec63p, suggest that biogenesis of PC1 and PC2 (among many other proteins) are affected in ADPLD. To examine the role of ADPLD genes in the biogenesis of polycystins, we used conditionally immortalized epithelial cell lines produced from kidney tubules of *Prkcsh*$^{flox/flox}$; *pCX-CreER*; *Pkd1*$^{F/H}$-BAC, *Sec63*$^{flox/flox}$ and *Sec63*$^{flox/flox}$; *Pkd1*$^{F/H}$-BAC mice. Tamoxifen induction (for the *Prkcsh* cell lines) or transient expression of Cre recombinase (for *Sec63* cell lines) produced null cells for the respective genes (Fig. 1a). PC1 expressed from the *Pkd1*$^{F/H}$-BAC transgene is cleaved into an N-terminal fragment and a C-terminal fragment (CTF), with little residual full-length PC1 remaining *in vivo* (Fig. 1e)[40]. This allowed us to use the HA-epitope–tagged CTF to monitor PC1 expression (Fig. 3). *Prkcsh*$^{-/-}$ cells showed a twofold decrease in steady state levels of PC1 (Fig. 3a). Kidney tissue from *Prkcsh*$^{flox/flox}$; *Ksp-Cre*; *Pkd1*$^{F/H}$-BAC mice also showed markedly decreased expression of PC1, thereby extending the cell-based findings to tissue *in vivo* (Supplementary Fig. 3a). *Sec63*-null cells showed similar decreases in PC1 expression (Supplementary Fig. 3b). *Prkcsh*$^{-/-}$ cells and *Prkcsh*$^{flox/flox}$; *Ksp-Cre* cystic kidney tissues had moderately decreased levels of PC2 expression (Fig. 3b); *Sec63* null cells and tissues also showed similarly decreased PC2 expression (Supplementary Fig. 3d). GIIβ and Sec63p function in generalized protein biosynthetic pathways, and expression of other integral membrane proteins was also affected by the loss of either gene product. For example, NaK-ATPase was reduced in null cells and cystic kidneys from *Prkcsh* and *Sec63* mutants; the ER resident integral membrane protein calnexin was unchanged (Supplementary Fig. 3c,d).

The quantitative decrease in PC1 expression in *Prkcsh*$^{-/-}$; *Pkd1*$^{F/H}$-BAC null cells (Fig. 3a) is not different from that expected in the *Pkd1*$^{+/-}$ heterozygous state and is unlikely to be sufficient to cause cysts[41]. We therefore hypothesized that cyst formation in the setting of defective GIIβ activity results from functional impairment of the residual PC1 protein. To assess such functional defects, we first examined the resistance of PC1 to digestion by endoglycosidase H (Endo H). Resistance to Endo H is an indicator of trafficking to the cell surface. PC1-CTF in *Prkcsh*-null cells showed substantial reduction in the fraction of proteins resistant to Endo H (Fig. 3c), indicating that little of the residual PC1 traffics past the middle Golgi in the absence of GIIβ. The primary cilium has been proposed[26] as the main site of action for PC1 and PC2. Because global measures of the cellular expression and glycosylation status of polycystins may not fully reflect the effects on polycystin function in the minute ciliary compartment, we examined the expression of PC1 and PC2 in the cilia of *Prkcsh*-null cells. Native PC2 expression was not discernibly different in the cilia of *Prkcsh*$^{flox/flox}$; *Pkd1*$^{F/H}$-BAC and *Prkcsh*$^{-/-}$; *Pkd1*$^{F/H}$-BAC cells (Fig. 3d). PC2 expression was also unchanged in *Sec63*$^{-/-}$ cells compared to *Sec63*$^{flox/flox}$ cells (Supplementary Fig. 4). PC1 expressed from the *Pkd1*$^{F/H}$-BAC transgene was readily detectable in cilia of *Prkcsh*$^{flox/flox}$; *Pkd1*$^{F/H}$-BAC cells using HA antibodies (Fig. 3e and Supplementary Fig. 5).

However, cilia of *Prkcsh*$^{-/-}$; *Pkd1*$^{F/H}$-BAC cells showed markedly reduced or absent expression of PC1 when compared to *Prkcsh*$^{flox/flox}$; *Pkd1*$^{F/H}$-BAC cells (Fig. 3e and Supplementary Fig. 5). As the *Pkd1*$^{F/H}$-BAC transgene rescues the cystic phenotype *in vivo*, it is likely that this markedly reduced expression level is sufficient for the functional rescue we observed and that the occasional apparent absence of PC1 in cilia by immunofluorescence represents the limitation of our detection. The data show that absence of GIIβ substantially impairs trafficking of PC1 to cilia and suggest that, without transgenic overexpression, the amount of PC1 reaching the cilia is not sufficient to avert cyst formation in ADPLD.

Given the markedly reduced amount of PC1 in cilia even in the setting of BAC transgenic overexpression (Fig. 3e), we examined whether the rescue of the cystic phenotypes by overexpressed PC1 was durable. *Prkcsh*$^{flox/flox}$ ; *Ksp-Cre*; *Pkd1*$^{F/H}$-BAC kidneys remained non-cystic at 3 months, whereas the *Pkd2*-BAC transgene did not slow cyst progression (Fig. 4a,b). Microscopically discernible tubular dilation and mild cyst formation did appear at 6 months in *Prkcsh*$^{flox/flox}$; *Ksp-Cre*; *Pkd1*$^{F/H}$-BAC kidneys, suggesting a marked slowing rather than a complete cessation of expansion in luminal diameter (Fig. 4c). In keeping with the more severe effect of loss of *Sec63*, we saw a similar but earlier emergence of delayed mild cyst formation with *Sec63*$^{flox/flox}$; *Ksp-Cre*; *Pkd1*$^{F/H}$-BAC mice at P45 (Fig. 4d). In aggregate, these combinatorial genetic data indicate that *Prkcsh* and *Sec63* mediate cystic disease by effectively reducing functional PC1 protein dosage. We show that tubule diameter from mild dilation to cyst formation is a continuously modulated trait determined by PC1 function in a dosage- and time-dependent manner, with an absolute requirement for the presence of functional PC2.

## The effects of reduced PC1 dosage differ by nephron segment

*Ksp-Cre* is active in TAL and the collecting duct segments of the nephron[33,34]. In both *Prkcsh* and *Sec63* cystic kidneys, the collecting duct formed large cysts, whereas TAL tubules were dilated to a lesser extent (Fig. 5). This greater severity of collecting duct cysts is similar to the observations in *Pkd1*$^{flox/flox}$; *Ksp-Cre* and *Pkd2*$^{WS25/-}$ mice[29,34]. However, conclusions regarding segment-specific sensitivity in these models were potentially confounded by segment-specific differences in either *Ksp-Cre* activity or somatic second hits, respectively. We took advantage of the additive contribution to cyst formation of the *Pkd1*$^{+/-}$ background in ADPLD to evaluate segment-specific sensitivity to *Pkd1* dosage without these potential confounding factors. Combination of *Prkcsh* or *Sec63* cystic kidney models with *Pkd1*$^{+/-}$ resulted in substantial increases in collecting duct cysts without an appreciable change in TAL tubule dilation (Fig. 5e,f,k,l). This indicates that reduced dosage of PC1 increases the severity of PKD primarily through increased growth of collecting duct cysts. We next examined the relative contributions of PC1 dosage-dependent proliferation and apoptosis to collecting duct cyst growth in *Prkcsh*$^{flox/flox}$; *Ksp-Cre* and *Sec63*$^{flox/flox}$; *Ksp-Cre* kidneys. The *Pkd1*$^{+/-}$ background significantly increased both proliferation (Fig. 5m–p,u) and apoptosis (Fig. 5q–t,u) in the collecting duct cysts of the ADPLD models; increased proliferation appears to predominate (Fig. 5u). These data provide evidence for segment-specific differences in cyst progression in ADPKD[29,34] and show that reduced dosage of PC1 facilitates cyst growth through enhanced net proliferation in a manner similar to that seen following complete loss[34].

## PC1 dosage modifies the severity of ARPKD

*Pkhd1*$^{del4/del4}$ mice develop a liver phenotype typical of ARPKD and have loss of oriented cell division in elongating tubules but do not develop kidney cysts, perhaps because of residual hypomorphic FPC acitivty[20,42]. FPC is a client protein for Sec63p and GIIβ, so we examined the interaction between *Pkhd1*$^{del4}$ and *Sec63* with the premise that inactivation of

Sec63 will eliminate any residual activity of the hypomorphic *Pkhd1*$^{del4}$ gene product (Fig. 6). *Sec63*$^{flox/flox}$; *Ksp-Cre*; *Pkhd1*$^{del4/del4}$ mice developed a more severe cystic disease than *Sec63*$^{flox/flox}$; *Ksp-Cre* mice (Fig. 6a–c), but their disease was not as severe as that of *Sec63*$^{flox/flox}$; *Ksp-Cre*; *Pkd1*$^{+/-}$ mice (Supplementary Fig. 6). There was no increase in cyst severity in *Sec63*$^{flox/flox}$; *Ksp-Cre*; *Pkhd1*$^{del4/+}$ mice (data not shown). Increased cyst formation in *Sec63*$^{flox/flox}$; *Ksp-Cre*; *Pkhd1*$^{del4/del4}$ mice was confined to collecting duct cysts in a pattern that recapitulates findings in *Sec63*$^{flox/flox}$; *Ksp-Cre*; *Pkd1*$^{+/-}$ mice and in human ARPKD (Fig. 6d). Because there is evidence of genetic interaction between *Pkhd1* and *Pkd1* (Supplementary Fig. 7a–c)[43], we overexpressed PC1 in an effort to separate the interaction of *Pkhd1* with *Pkd1* from interaction with *Sec63*. The *Pkd1*$^{F/H}$-BAC transgene markedly rescued the cystic phenotype of *Sec63*$^{flox/flox}$; *Ksp-Cre*; *Pkhd1*$^{del4/del4}$ mice; the residual microscopic cystic disease was much less severe than that seen in *Sec63*$^{flox/flox}$; *Ksp-Cre* alone (Fig. 6a–c). This minimal residual disease may be the result of a persistently sensitized background resulting from functional hypomorphism of PC1 even after transgenic re-expression (for example, Figs. 3e and 4d) and is consistent with the observation that even *Pkd1* haploinsufficiency is sufficient to elicit phenotypes in the presence of mutations in *Pkhd1* that otherwise do not show kidney cysts (Supplementary Fig. 7a,b)[43]. We also found that reduced PC1 dosage in *Pkhd1*$^{del4/del4}$; *Pkd1*$^{+/-}$ mice worsened the liver phenotype compared to *Pkhd1*$^{del4/del4}$ alone; however, PC1 overexpression in *Pkhd1*$^{del4/del4}$; *Pkd1*$^{F/H}$-BAC mice had no beneficial effect on liver disease (Supplementary Fig. 7c). Finally, reduced dosage of PC2 by the *Pkd2*$^{+/-}$ background had no effect on the *Pkhd1*$^{del4/del4}$ phenotype, supporting the role of PC1 as the rate-limiting factor (Supplementary Fig. 7d,e). The most consistent interpretation of these data is that reduced dosage of PC1 sensitizes kidney tubules and bile ducts to expression of phenotypes resulting from alterations in FPC.

## Proteasome inhibitor therapy in ADPLD

Mutations in *Prkcsh* and *Sec63* result in impaired protein biogenesis and quality control and lead to formation of misfolded proteins that undergo retro-translocation and degradation using proteasome-mediated mechanisms[44]. Under this formulation, inhibition of the proteasome may increase the unfolded protein burden to toxic levels, leading to increased sensitivity of cyst cells to proteasome inhibitor therapy. In keeping with this hypothesis, we found that *Prkcsh*$^{-/-}$; *Pkd1*$^{F/H}$-BAC cells showed significantly higher rates of apoptosis following treatment with the proteasome inhibitors MG132 and carfilzomib compared to cells with normal expression of GIIβ (Fig. 7a and Supplementary Fig. 8). In addition, MG132 significantly increased steady-state levels of PC1 in *Prkcsh*$^{-/-}$; *Pkd1*$^{F/H}$-BAC cells, presumably by inhibiting degradation of residual PC1 (Fig. 7b). These findings suggest that protea-some inhibition may slow cyst progression in ADPLD by increasing cyst-lining cell apoptosis and by decreasing PC1-dependent proliferation (Fig. 7). We treated severely cystic *Prkcsh*$^{flox/flox}$; *Ksp-Cre*; *Pkd1*$^{+/-}$ mice with the irreversible proteasome inhibitor carfilzomib (5 mg/kg) intravenously twice weekly for 3 weeks beginning at P21 (Fig. 7c,e and Supplementary Fig. 9). The efficacy of this regimen was evidenced by increased levels of Hif1 α in the kidneys of treated mice (Fig. 7c). Carfilzomib treatment significantly reduced the kidney weight to body weight ratio, the cystic index and BUN when compared to vehicle-treated controls (Fig. 7e). The rate of apoptosis in cyst-lining cells of *Prkcsh*$^{flox/flox}$; *Ksp-Cre;Pkd1*$^{+/-}$ mice was increased with carfilzomib treatment, whereas the rate of proliferation was decreased (Fig. 7g). We also tested this therapy in less severely affected *Prkcsh*$^{flox/flox}$; *Ksp-Cre* mice, which have a genotype more akin to the human disease. *Prkcsh*$^{flox/flox}$; *Ksp-Cre* mice treated with weekly carfilzomib for 6 weeks beginning at P42 showed an even more profound improvement in cyst progression (Fig. 7d,f and Supplementary Fig. 9). Neither mouse model showed adverse effects from proteasome inhibition during treatment. In aggregate, these data suggest that inhibition of proteasome function can improve the course of ADPLD in the orthologous animal models.

## DISCUSSION

Sec63p and GIIβ are components of the ER translocation, folding and quality control machinery through which 30% of proteins encoded by the human genome pass, yet heterozygous mutations in these genes manifest only with bile duct cysts indistinguishable from the liver phenotype in ADPKD[1]. Although biochemical and cell biological studies may offer clues, a comprehensive understanding of the genetic and functional interrelationships that define this system requires the use of orthologous gene-based *in vivo* mammalian models. Our findings using the latter approach place PC1 at the center of three human polycystic diseases. We produced a spectrum of cystic disease severity using combinations of mutant and overexpression alleles to define the functional interrelationships between five genes: *Prkcsh*, *Sec63*, *Pkd1*, *Pkd2* and *Pkhd1*. Cyst formation in all combinations of these genes, except complete loss of *Pkd2*, can be significantly modulated by altering expression of *Pkd1*, indicating that PC1 is the rate-limiting component in cyst formation in human ADPLD, ADPKD and ARPKD.

Despite their phenotypic similarities and functional dependence on *Pkd1*, the mechanisms differ among the three diseases in the current study. In contrast to ADPKD, in which disease typically results from complete somatic loss of *Pkd1* or *Pkd2*, the ADPLD gene orthologs *Prkcsh* and *Sec63* cause cysts by profoundly reducing expression and effective trafficking of functionally active PC1. Evidence for a possible gene-dosage effect for polycystins was first described in *trans* heterozygous states in humans[45] and mice[41]. More recently, mutations in *Pkd1* resulting in reduction of functional PC1 have suggested that reduced activity is sufficient to cause cyst formation in some situations[46–48]. Our data define a more complex relationship. The variables that determine tubule dilation and cyst formation include the level of PC1 expression, the threshold below which progressive tubule dilation can begin, the degree to which PC1 activity falls below this threshold and the activity of other factors that determine the extent of response once tubule dilation and cyst formation is initiated. The quantitative features of these determinants are likely to vary between bile ducts and kidney tubules and between different segments and cell types within kidney tubules. These differences may underlie the liver-specific findings in ADPLD compared to the kidney predominance in ADPKD. We hypothesize that in individuals with ADPLD, somatic loss of either *SEC63* or *PRKCSH* may occur in either kidney tubules or bile ducts. The basis for the clinical difference in ADPLD and ADPKD may be that, in ADPLD, the ensuing decrease in PC1 activity in bile ducts falls to a level sufficient to cause PLD, but the decrease in PC1 activity in kidney tubules is not sufficient to cause PKD.

Our data show another feature of cyst formation. The threshold and rate for cyst growth is not a binary on-off process but rather a continuously regulated process. Reducing PC1 levels with *Prkcsh* mutation alone results in cyst growth; further reducing the equilibrium of the PC1-PC2 functional complex by combining *Prkcsh* mutation with the $Pkd2^{+/-}$ background increases the rate of cyst growth. A more profound increase in cyst growth is seen on the $Pkd1^{+/-}$ background. These findings suggest that the farther below the threshold PC1-PC2 activity falls, the greater the rate of tubule dilation and cyst growth. The increased cyst formation in *Sec63*; *Prkcsh* double knockouts further supports this conclusion. None of these models grow cysts as rapidly as the model with complete inactivation of *Pkd1* (ref. 34), so the continuum of cyst growth rates shows a substantial amount of dynamism. The differences in the rate of cyst growth between the collecting duct and TAL on the $Pkd1^{+/+}$ and $Pkd1^{+/-}$ backgrounds suggest that specific cell types can have different responses to PC1-dependent signal dosage variation.

We found that a *Pkhd1* mutation that does not result in a kidney phenotype in mice nonetheless results in worsened kidney cysts when combined with mutation of *Sec63*. The

kidney cysts in the *Pkhd1*; *Sec63* mice were largely rescued by PC1 overexpression, supporting the conclusion that reduced PC1 dosage sensitizes mice with mutations in *Pkhd1* to polycystic kidney phenotypes. The *Pkhd1*$^{del4}$ mutation causes loss of oriented cell division without cyst formation[42]. It is possible that, when coupled with a propensity toward proliferation resulting from reduced PC1 dosage, *Pkhd1*-dependent defects in oriented cell division are sufficient to exacerbate cyst growth in mice. The inability of PC1 overexpression to improve the liver phenotype in *Pkhd1*$^{del4/del4}$ mice suggests that *Pkhd1* also has PC1-independent functions in bile ducts. It is possible that the functional relationship between PC1 and FPC is conserved between humans and mice. A plausible hypothesis for the observed species differences in the ARPKD kidney phenotype may be that the normal level of PC1 expression in humans is closer to the threshold for eliciting a *PKHD1* mutant phenotype than it is in mice.

The finding that proteasome inhibitor therapy is effective in our orthologous model of ADPLD offers a conceptual therapeutic approach to ADPLD. The clinical utility of this approach will need to be tempered by the side effect profile relative to potential benefit, but the heightened sensitivity of cells with mutations in the ADPLD genes to proteasome inhibition may offer an improved therapeutic index in this regard. We observed decreased degradation of improperly processed PC1 following proteasome inhibition. In light of this and the acute sensitivity of cyst formation to PC1 'dose', investigation of the utility of proteasome inhibition in orthologous models of ADPKD based on hypomorphic and amino acid substitution variants of *Pkd1* may be warranted.

## ONLINE METHODS

### Mouse lines and treatments

All experiments were conducted in accordance with Yale University Institutional Animal Care and Use Committee guidelines and procedures. The conditional *flox* mice were made in 129/Sv embryonic stem cells, and chimeras were mated to C57BL6 for germline transmission. The BAC transgenic lines were produced in (C57BL/6J X SJL/J) F2, and germline transmission was achieved by mating to C57BL6. All strains were subsequently backcrossed at least four generations with C57BL6 and are therefore expected to be at least 90% C57BL6 congenic. Mice of both sexes were used in this study. We generated the conditional allele *Prkcsh*$^{flox}$ with the *loxP* sites flanking exons 6 and 7 with a *neo* selection cassette flanked by the FRT site located in IVS7. Deletion of exons 6 and 7 by Cre recombinase results in a functionally null allele (for example, Fig. 3a and data not shown). We generated a conditional *Sec63*$^{flox}$ allele with *loxP* sites flanking exon 2 and a *neo* cassette flanked by FRT sites inserted into IVS2. Removal of exon 2 by Cre recombinase activity results in complete loss of function (for example, Supplementary Fig. 3b and data not shown). *Pkd1*$^{F/H}$-BAC was generated by modification of the *Pkd1*-containing BAC clone RPCI22-287A3 using a previously used method[49] to introduce three copies of HA before the stop codon and three copies of FLAG after the leader sequence. Purified insert from the modified BAC was used for pronuclear injection to generate multiple transgenic founder lines. Founders were validated for copy number by genomic quantitative PCR and the ability to completely rescue the embryonic lethal null phenotype in *Pkd1*$^{-/-}$ mice. The current study used founder Tg248, which has three copies of the BAC transgene. The other mouse lines used have been previously published: *Pkd1*$^{flox}$ (ref. 34), *Pkd2*$^{flox}$ (ref. 31), *Pkd1*$^{+/-}$ (ref. 41), *Pkd2*$^{+/-}$ (ref. 50), *Pkhd1*$^{del4}$ (ref. 20), *Pkd2*-BAC[36], *Ksp-Cre*[33], *pCX-Cre* (*pCAGGS*)[51] and *Pkhd1-Cre*[52].

### Drug treatments

Inducible Cre expression (*pCX-Cre*) was begun at P28 with intraperitoneal injections of 0.1 mg/g/day of tamoxifen suspended in sunflower seed oil and administered for 5 days; livers were harvested at P90. The proteasome inhibitor carfilzomib (5 mg/kg) was administered intravenously in the tail vein twice weekly for 3 weeks beginning at P21 for *Prkcsh*$^{flox/flox}$; *Ksp-Cre*; *Pkd1*$^{+/-}$ mice and once weekly for 6 weeks beginning at P42 for *Prkcsh*$^{flox/flox}$; *Ksp-Cre* mice.

### Prkcsh and Sec63 mutant cell lines

*Prkcsh*$^{flox/flox}$; *pCX-Cre*, *Sec63*$^{flox/flox}$ and *Sec63*$^{flox/flox}$; *Pkd1*$^{F/H}$-BAC mice were intercrossed with the ImmortoMouse interferon-γ inducible H-2K$^{b}$-tsA58 SV40 temperature-sensitive transgenic line, and kidney tubule epithelial cell lines were produced as described previously[34]. Resultant 'parental' cell lines were converted to null cell lines *ex vivo* either by treatment with 200 nM 4-hydroxytamoxifen (4 days) for *Prkcsh*$^{flox/flox}$; *pCX-Cre* cell lines or by transient transfection with Cre-recombinase plasmid followed by cloning using limiting dilution cloning for *Sec63*$^{flox/flox}$ and *Sec63*$^{flox/flox}$; *Pkd1*$^{F/H}$-BAC cells. Control cells were those in which Cre recombinase was not activated. Prior to the experiments, cells were allowed to differentiate following silencing of the SV40 large T antigen under non-permissive conditions (37 °C, without interferon-γ for 7–21 days.

### Immunohistochemistry and immunocytochemistry

Mice were anaesthetized by an intraperitoneal injection of ketamine/xylazine and fixed *in situ* by perfusion through the heart with 4% paraformaldehyde in 1 × PBS for 3 min. Sections (5–7 μm) were used for immunohistochemical studies according to standard procedures[34]. Cells were cultured on collagen coated glass cover slips or on semipermeable membrane supports for 10–21 days at the non-permissive temperature (37 °C) in the absence of γ-interferon to allow the cells to differentiate and polarize. Immunoblotting and immunoprecipitation of tissues and cells were performed as described previously[34]. Analysis of the immunofluorescent staining as well as quantitation of cystic indices were carried out using a Nikon TE2000U microscope and MetaMorph software[34].

### Primary antibodies and lectins

The following antibodies and lectins were used: fluorescein-labeled *Lotus tetragonolobus* lectin (LTA, Vector Laboratories); fluorescein-*Dolichos biflorus* agglutinin (DBA, Vector Laboratories); sheep anti-Tamm-Horsfall protein (THP, Biotrend Chemicals); mouse anti-acetylated α-tubulin (Sigma); rabbit anti-PC2 (YCC2)[53]; rabbit anti-HA (Zymed Laboratories); mouse anti-$Na^{+}$,$K^{+}$-ATPase (clone 6H; kind gift from M. Caplan, Yale University); rabbit anti-GIIβ (kind gift from J. Roth, University of Zurich); rabbit anti-Sec63 (kind gift from R. Zimmermann, Saarland University, Homburg, Germany); rabbit anti-Ki67 (Vector Labs); mouse anti-BrdU (Sigma); rabbit anti-calnexin (Stressgen).

### Protein preparation and protein blot analysis

Tissues were extracted and homogenized with a motor driven Teflon pestle homogenizer in ice-cold buffer (250 mM sucrose, 1 mM EGTA, 25 mM Tris at pH 7.4 containing protease inhibitors). The homogenates were centrifuged twice at 500*g*. The resulting supernatant was analyzed as total lysate. Cells were harvested and lysed in RIPA buffer or in PC1 cleavage buffer (20 mM sodium phosphate at pH 7.2, 150 mM NaCl, 1 mM EDTA, 10% (vol/vol) glycerol, 0.5% Triton X-100) containing complete protease inhibitor cocktails (Roche Molecular Biochemicals) for 30 min on ice. The lysate was cleared by centrifugation for 10 min at 4 °C. All protein samples were quantitated using the Bradford assay and electrophoresed on a 3–8% gradient gel (Novex Tris Acetate gels, Invitrogen) for the analysis of

proteins larger than 200 kDa and 10% gels for proteins with sizes between 30–200 kDa (Tris-glycine gels, Bio-Rad). The proteins were electroblotted to a poly-vinylidene difluoride (PVDF) membrane overnight and probed with various antibodies.

### Immunoprecipitation

For detection of PC-1 cleavage, cell lysates (30–80 μg of protein) were incubated with mouse anti-HA pre-conjugated agarose beads (Sigma) at 4 °C overnight under rotation. The beads were washed three times the next day with lysis buffer (20 mM sodium phosphate, pH 7.2, 150 mM NaCl, 1 mM EDTA, 10% (vol/vol) glycerol, 0.5% Triton X-100) containing complete protease inhibitor cocktails (Roche Molecular Biochemicals). The beads were then boiled for 5 min in 2× SDS loading dye, followed by SDS-PAGE and protein blotting with rabbit HA antisera.

### Proteasome inhibition

MG132 (Sigma) or carfilzomib (Proteolix) was added to the media of cells 6–16 h before immunostainig or lysis prior to, immuno-precipitation and anti-HA protein blotting.

### Proliferation and apoptosis

Mice received intraperitoneal injections of bromo-deoxyuridine (BrdU) dissolved in saline (25 mg/kg) daily for 5 days or as a single dose 3 h before perfusion fixation. Immunohistochemistry was performed using mouse BrdU monoclonal antibody. Alternatively, proliferation was assayed by anti-Ki67 immunostaining. Apoptosis analysis was carried out by TUNEL staining according to the manufacturer's instructions (Roche). Sections were also stained with DAPI and DBA, and the number of BrdU- or TUNEL-positive nuclei in at least 1,000 DBA-positive nuclei per kidney were counted to determine the rates for proliferation and apoptosis, respectively.

### Statistical analysis

Comparisons of three or more groups were performed using ANOVA followed by Tukey's multiple group comparison post test. The comparison of two groups was performed using the two-tailed Student's *t*-test. A value of $P < 0.05$ was considered significant. Data are presented as mean ± standard error (s.e.m.).

## Supplementary Material

Refer to Web version on PubMed Central for supplementary material.

## Acknowledgments

Carfilzomib was a kind gift from Proteolix, Inc. This work was supported by grants from the National Institute of Diabetes and Digestive and Kidney Disease (NIDDK)/ US National Institutes of Health (NIH) (R01DK51041 and R01DK54053 to S.S. and F31DK083904 to S.V.F.) and a grant from the Mizutani Foundation for Glycoscience (S.S.). We are grateful for support from the Nephrology Training Grant (T32DK007276) to S.V.F. and the Joseph LeRoy and Ann C. Warner Fund (S.S.). The authors are members of the Yale PKD Center (P50DK57328). We are grateful for Core services from the Yale O'Brien Kidney Center (P30DK079310).

## References

1. Qian Q, et al. Clinical profile of autosomal dominant polycystic liver disease. Hepatology. 2003; 37:164–171. [PubMed: 12500201]
2. Reynolds DM, et al. Identification of a locus for autosomal dominant polycystic liver disease, on chromosome 19p13.2-13.1. Am. J. Hum. Genet. 2000; 67:1598–1604. [PubMed: 11047756]

3. Li A, et al. Mutations in *PRKCSH* cause isolated autosomal dominant polycystic liver disease. Am. J. Hum. Genet. 2003; 72:691–703. [PubMed: 12529853]
4. Davila S, et al. Mutations in *SEC63* cause autosomal dominant polycystic liver disease. Nat. Genet. 2004; 36:575–577. [PubMed: 15133510]
5. Drenth JP, Te Morsche RH, Smink R, Bonifacino JS, Jansen JB. Germline mutations in *PRKCSH* are associated with autosomal dominant polycystic liver disease. Nat. Genet. 2003; 33:345–347. [PubMed: 12577059]
6. Lyman SK, Schekman R. Binding of secretory precursor polypeptides to a translocon subcomplex is regulated by BiP. Cell. 1997; 88:85–96. [PubMed: 9019409]
7. Young BP, Craven RA, Reid PJ, Willer M, Stirling CJ. Sec63p and Kar2p are required for the translocation of SRP-dependent precursors into the yeast endoplasmic reticulum *in vivo*. EMBO J. 2001; 20:262–271. [PubMed: 11226176]
8. Misselwitz B, Staeck O, Matlack KE, Rapoport TA. Interaction of BiP with the J-domain of the Sec63p component of the endoplasmic reticulum protein translocation complex. J. Biol. Chem. 1999; 274:20110–20115. [PubMed: 10400622]
9. Trombetta ES, Simons JF, Helenius A. Endoplasmic reticulum glucosidase II is composed of a catalytic subunit, conserved from yeast to mammals, and a tightly bound noncatalytic HDEL-containing subunit. J. Biol. Chem. 1996; 271:27509–27516. [PubMed: 8910335]
10. Trombetta ES, Fleming KG, Helenius A. Quaternary and domain structure of glycoprotein processing glucosidase II. Biochemistry. 2001; 40:10717–10722. [PubMed: 11524018]
11. Helenius A, Aebi M. Roles of N-linked glycans in the endoplasmic reticulum. Annu. Rev. Biochem. 2004; 73:1019–1049. [PubMed: 15189166]
12. Stigliano ID, Caramelo JJ, Labriola CA, Parodi AJ, D'Alessio C. Glucosidase II β subunit modulates N-glycan trimming in fission yeasts and mammals. Mol. Biol. Cell. 2009; 20:3974–3984. [PubMed: 19605557]
13. The European Polycystic Kidney Disease Consortium. The polycystic kidney disease 1 gene encodes a 14 kb transcript and lies within a duplicated region on chromosme 16. Cell. 1994; 77:881–894. [PubMed: 8004675]
14. The International Polycystic Kidney Disease Consortium. Polycystic kidney disease: The complete structure of the *PKD1* gene and its protein. Cell. 1995; 81:289–298. [PubMed: 7736581]
15. Mochizuki T, et al. *PKD2*, a gene for polycystic kidney disease that encodes an integral membrane protein. Science. 1996; 272:1339–1342. [PubMed: 8650545]
16. Pazour GJ, San Agustin JT, Follit JA, Rosenbaum JL, Witman GB. Polycystin-2 localizes to kidney cilia and the ciliary level is elevated in *orpk* mice with polycystic kidney disease. Curr. Biol. 2002; 12:R378–R380. [PubMed: 12062067]
17. Yoder BK, Hou X, Guay-Woodford LM. The polycystic kidney disease proteins, polycystin-1, polycystin-2, polaris, and cystin, are co-localized in renal cilia. J. Am. Soc. Nephrol. 2002; 13:2508–2516. [PubMed: 12239239]
18. Nauli SM, et al. Polycystins 1 and 2 mediate mechanosensation in the primary cilium of kidney cells. Nat. Genet. 2003; 33:129–137. [PubMed: 12514735]
19. Ward CJ, et al. Cellular and subcellular localization of the ARPKD protein; fibrocystin is expressed on primary cilia. Hum. Mol. Genet. 2003; 12:2703–2710. [PubMed: 12925574]
20. Gallagher AR, et al. Biliary and pancreatic dysgenesis in mice harboring a mutation in *Pkhd1*. Am. J. Pathol. 2008; 172:417–429. [PubMed: 18202188]
21. Wang S, Zhang J, Nauli SM, Starremans P, Zhou J. Fibrocystin is associated with polycystin-2 and regulates intracellular calcium. J. Am. Soc. Nephrol. 2004; 15:12A.
22. Smith UM, et al. The transmembrane protein meckelin (MKS3) is mutated in Meckel-Gruber syndrome and the wpk rat. Nat. Genet. 2006; 38:191–196. [PubMed: 16415887]
23. Sharma N, Berbari NF, Yoder BK. Ciliary dysfunction in developmental abnormalities and diseases. Curr. Top. Dev. Biol. 2008; 85:371–427. [PubMed: 19147012]
24. Qian F, et al. Cleavage of polycystin-1 requires the receptor for egg jelly domain and is disrupted by human autosomal-dominant polycystic kidney disease 1-associated mutations. Proc. Natl. Acad. Sci. USA. 2002; 99:16981–16986. [PubMed: 12482949]

25. Kaimori JY, et al. Polyductin undergoes notch-like processing and regulated release from primary cilia. Hum. Mol. Genet. 2007; 16:942–956. [PubMed: 17470460]
26. Menezes LF, Germino GG. Polycystic kidney disease, cilia, and planar polarity. Methods Cell Biol. 2009; 94:273–297. [PubMed: 20362096]
27. Qian F, Watnick TJ, Onuchic LF, Germino GG. The molecular basis of focal cyst formation in human autosomal dominant polycystic kidney disease type I. Cell. 1996; 87:979–987. [PubMed: 8978603]
28. Watnick TJ, et al. Somatic mutation in individual liver cysts supports a two-hit model of cystogenesis in autosomal dominant polycystic kidney disease. Mol. Cell. 1998; 2:247–251. [PubMed: 9734362]
29. Wu G, et al. Somatic inactivation of *Pkd2* results in polycystic kidney disease. Cell. 1998; 93:177–188. [PubMed: 9568711]
30. Piontek K, Menezes LF, Garcia-Gonzalez MA, Huso DL, Germino GG. A critical developmental switch defines the kinetics of kidney cyst formation after loss of *Pkd1*. Nat. Med. 2007; 13:1490–1495. [PubMed: 17965720]
31. Spirli C, et al. ERK1/2-dependent vascular endothelial growth factor signaling sustains cyst growth in polycystin-2 defective mice. Gastroenterology. 2010; 138:360–371. [PubMed: 19766642]
32. Van Keimpema L, et al. Patients with isolated polycystic liver disease referred to liver centres: clinical characterization of 137 cases. Liver Int. 2011; 31:92–98. [PubMed: 20408955]
33. Shao X, Somlo S, Igarashi P. Epithelial-specific Cre/lox recombination in the developing kidney and genitourinary tract. J. Am. Soc. Nephrol. 2002; 13:1837–1846. [PubMed: 12089379]
34. Shibazaki S, et al. Cyst formation and activation of the extracellular regulated kinase pathway after kidney specific inactivation of *Pkd1*. Hum. Mol. Genet. 2008; 17:1505–1516. [PubMed: 18263604]
35. Cao Y, et al. Chemical modifier screen identifies HDAC inhibitors as suppressors of PKD models. Proc. Natl. Acad. Sci. USA. 2009; 106:21819–21824. [PubMed: 19966229]
36. Geng L, et al. Syntaxin 5 regulates the endoplasmic reticulum channel-release properties of polycystin-2. Proc. Natl. Acad. Sci. USA. 2008; 105:15920–15925. [PubMed: 18836075]
37. Gao H, et al. PRKCSH/80K-H, the protein mutated in polycystic liver disease, protects polycystin-2/TRPP2 against HERP-mediated degradation. Hum. Mol. Genet. 2010; 19:16–24. [PubMed: 19801576]
38. Hanaoka K, et al. Co-assembly of polycystin-1 and -2 produces unique cation-permeable currents. Nature. 2000; 408:990–994. [PubMed: 11140688]
39. Yu Y, et al. Structural and molecular basis of the assembly of the TRPP2/PKD1 complex. Proc. Natl. Acad. Sci. USA. 2009; 106:11558–11563. [PubMed: 19556541]
40. Wodarczyk C, et al. A novel mouse model reveals that polycystin-1 deficiency in ependyma and choroid plexus results in dysfunctional cilia and hydrocephalus. PLoS ONE. 2009; 4:e7137. [PubMed: 19774080]
41. Wu G, et al. *Trans*-heterozygous *Pkd1* and *Pkd2* mutations modify expression of polycystic kidney disease. Hum. Mol. Genet. 2002; 11:1845–1854. [PubMed: 12140187]
42. Nishio S, et al. Loss of oriented cell division does not initiate cyst formation. J. Am. Soc. Nephrol. 2010; 21:295–302. [PubMed: 19959710]
43. Garcia-Gonzalez MA, et al. Genetic interaction studies link autosomal dominant and recessive polycystic kidney disease in a common pathway. Hum. Mol. Genet. 2007; 16:1940–1950. [PubMed: 17575307]
44. Vembar SS, Brodsky JL. One step at a time: endoplasmic reticulum-associated degradation. Nat. Rev. Mol. Cell Biol. 2008; 9:944–957. [PubMed: 19002207]
45. Pei Y, et al. Bilineal disease and *trans*-heterozygotes in autosomal dominant polycystic kidney disease. Am. J. Hum. Genet. 2001; 68:355–363. [PubMed: 11156533]
46. Jiang ST, et al. Defining a link with autosomal-dominant polycystic kidney disease in mice with congenitally low expression of *Pkd1*. Am. J. Pathol. 2006; 168:205–220. [PubMed: 16400024]
47. Lantinga-van Leeuwen IS, et al. Lowering of *Pkd1* expression is sufficient to cause polycystic kidney disease. Hum. Mol. Genet. 2004; 13:3069–3077. [PubMed: 15496422]

48. Rossetti S, et al. Incompletely penetrant *PKD1* alleles suggest a role for gene dosage in cyst initiation in polycystic kidney disease. Kidney Int. 2009; 75:848–855. [PubMed: 19165178]
49. Lalioti M, Heath J. A new method for generating point mutations in bacterial artificial chromosomes by homologous recombination in *Escherichia coli*. Nucleic Acids Res. 2001; 29:E14. [PubMed: 11160916]
50. Wu G, et al. Cardiac defects and renal failure in mice with targeted mutations in *Pkd2*. Nat. Genet. 2000; 24:75–78. [PubMed: 10615132]
51. Guo C, Yang W, Lobe CG. A Cre recombinase transgene with mosaic, widespread tamoxifen-inducible action. Genesis. 2002; 32:8–18. [PubMed: 11835669]
52. Patel V, et al. Acute kidney injury and aberrant planar cell polarity induce cyst formation in mice lacking renal cilia. Hum. Mol. Genet. 2008; 17:1578–1590. [PubMed: 18263895]
53. Cai Y, et al. Identification and characterization of polycystin-2, the *PKD2* gene product. J. Biol. Chem. 1999; 274:28557–28565. [PubMed: 10497221]

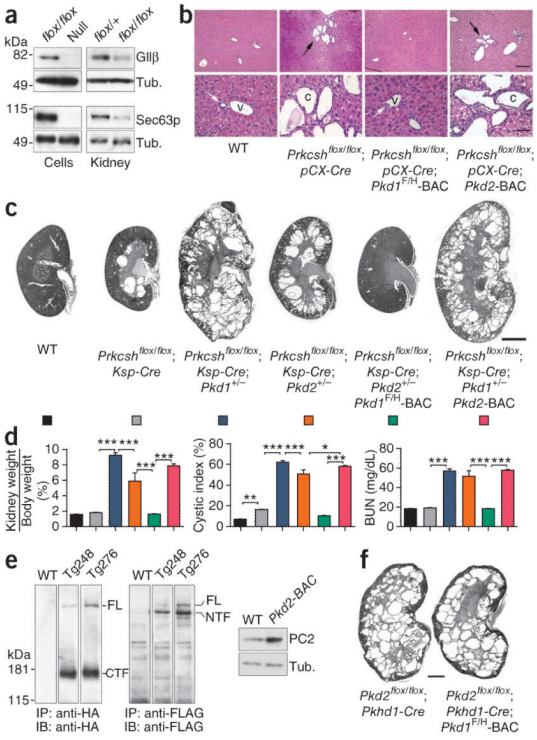


**Figure 1.**

Pkd1 dosage is the main genetic determinant of *Prkcsh*-dependent cyst formation. (**a**) Prkcsh$^{flox}$ (top) and *Sec63*$^{flox}$ (bottom) produce null alleles upon deletion. In the left panels, GIIβ and Sec63p disappear from kidney cell lines (*flox/flox*) following Cre expression (null). In the right panels, GIIβ and Sec63p are markedly reduced in mosaic *Prkcsh*$^{flox/flox}$; *Ksp-Cre* and *Sec63*$^{flox/flox}$; *Ksp-Cre* kidney tissue (*flox/flox*) compared to heterozygous controls. (**b**) *Prkcsh*$^{flox/flox}$; *pCX-CreER* mice, with inducible Cre expression in bile duct epithelia[31], develop liver cysts 8 weeks after treatment with tamoxifen from P28-P32 (black arrows). Expression of the *Pkd1*$^{F/H}$-BAC transgene, but not *Pkd2*-BAC, abrogates bile duct cyst formation (white arrows). v, venule; c, cyst. Scale bars, 500 μm in the upper panels and 100 μm in the lower panels. (**c**) The severity of cystic disease is markedly increased on the *Pkd1*$^{+/-}$ background and moderately increased on the *Pkd2*$^{+/-}$ background. The *Pkd1*$^{F/H}$-BAC transgene rescues the *Prkcsh*$^{flox/flox}$; *Ksp-Cre;Pkd2*$^{+/-}$ cystic phenotype; *Pkd2*-BAC has no effect. Ages, P42; scale bar, 2 mm. (**d**) Quantitative assessment of cyst severity by kidney weight to body weight ratio, cystic index and BUN. The colors of histogram bars correspond to the genotypes in **c**. $n = 7$ for each group except *Prkcsh*$^{flox/flox}$; *Ksp-Cre*; *Pkd1*$^{+/-}$, for which $n = 8$. Results are mean ± s.e.m. (ANOVA; ***P < 0.001, *P < 0.05). (**e**) Immunoblots with anti-HA (left) and anti-FLAG (middle) showing PC1 expression in membrane-enriched kidney tissue lysates from two representative *Pkd1*$^{F/H}$-BAC transgenic lines (Tg248 and Tg276). The majority of PC1 is cleaved *in vivo*. Tg248 was used in the current study. Transgenic PC2 overexpression in the liver of littermate mice (right). WT, non-transgenic. (**f**) Absence of phenotypic effect in *Pkd2*$^{flox/flox}$; *Pkhd1-Cre* mice with or without the *Pkd1*$^{F/H}$-BAC transgene (P21). Scale bar, 1 mm.

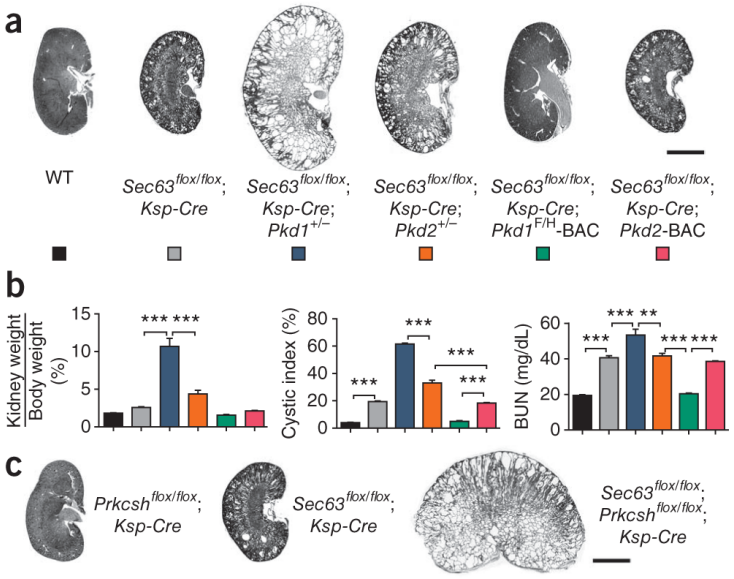


**Figure 2.**

*Pkd1* and *Pkd2* dosage in *Sec63*-dependent cyst formation. (**a,b**) Histological kidney sections (**a**) and aggregate data (**b**) from mice with the indicated genotypes at P21. The $Pkd1^{+/-}$ and $Pkd2^{+/-}$ backgrounds exacerbate cyst formation following loss of *Sec63*; the increase in severity is greater with $Pkd1^{+/-}$ than with $Pkd2^{+-}$. The $Pkd1^{F/H}$-BAC transgene rescues the PKD in $Sec63^{flox/flox}$; *Ksp-Cre* mice. The *Pkd2*-BAC transgene has no effect. Genotypes in the histograms (**b**) are indicated by the colors in **a**; *n* (from left to right) = 5, 8, 8, 9, 7, 5. Results are mean ± s.e.m. (ANOVA; ***P < 0.001, **P < 0.01). (**c**) $Sec63^{flox/flox}$; $Prkcsh^{flox/flox}$; *Ksp-Cre* doubly mutant mice show genetic interaction between *Prkcsh* and *Sec63*, with marked exacerbation of the cystic phenotype compared to either $Prkcsh^{flox/flox}$; *Ksp-Cre* or $Sec63^{flox/flox}$; *Ksp-Cre* mice at P21. Scale bar, 2 mm.

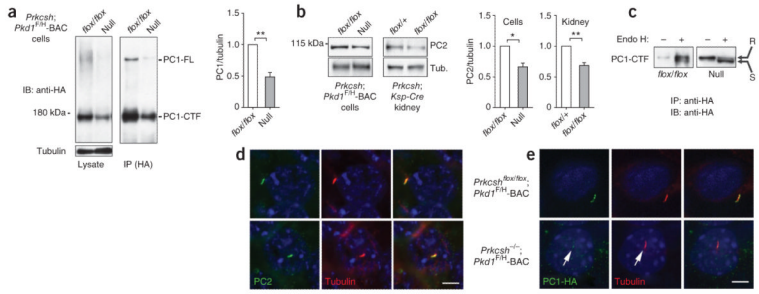


**Figure 3.**

Impaired biogenesis and trafficking of PC1 in ADPLD. (**a**) Immunoblots showing steady state expression of PC1 from the *Pkd1*$^{F/H}$-BAC transgene in *Prkcsh*$^{flox/flox}$; *Pkd1*$^{F/H}$-BAC (*flox/flox*) control and *Prkcsh*$^{-/-}$; *Pkd1*$^{F/H}$-BAC null cells lines. Left panel, immunoblot of total cell lysates with anti-HA; right panel, immunoblot following immunoprecipitation by anti-HA showing reduction in both the intramembranous PC1-CTF and uncleaved full-length PC1 (PC1-FL). Densitometric quantitation of PC1-CTF normalized to tubulin shows PC1 levels in null cells are ~48% of their respective controls ($n = 4$; $^{**}P = 0.0060$; results shown as mean ± s.e.m. (Student's *t*-test)). (**b**) Representative immunoblots showing PC2 expression in cell lines and kidney tissues. Densitometric quantitation normalized to tubulin shows that PC2 levels in null cells and cystic kidneys are reduced to ~66% of their respective controls ($n = 4$ for cell lines; $n = 3$ each for kidneys; $^{*}P = 0.0152$, $^{**}P = 0.0095$; mean ± s.e.m. (Student's *t*-test)). (**c**) Endo H resistant fraction (R, upper band) of PC1-CTF is markedly reduced and the Endo H sensitive fraction (S, lower band) is increased in *Prkcsh*$^{-/-}$; *Pkd1*$^{F/H}$-BAC cells (null) compared to *Prkcsh*$^{flox/flox}$; *Pkd1*$^{F/H}$-BAC controls (*flox/flox*), indicating reduced trafficking of PC1-CTF past the middle Golgi in null cells (**d,e**). Expression of PC2 (**d**) and PC1 (**e**) in cilia of *Prkcsh*$^{flox/flox}$; *Pkd1*$^{F/H}$-BAC control and *Prkcsh*$^{-/-}$; *Pkd1*$^{F/H}$-BAC null cells. PC2 trafficking to cilia is not altered by loss of GIIβ (**d**), whereas PC1 trafficking is markedly reduced in cilia (the arrow marks the weak PC1-HA signal) (**e**). Red, acetylated α-tubulin; green, anti-PC2 in **d** and anti-HA in **e**. Scale bar, 5 μm.

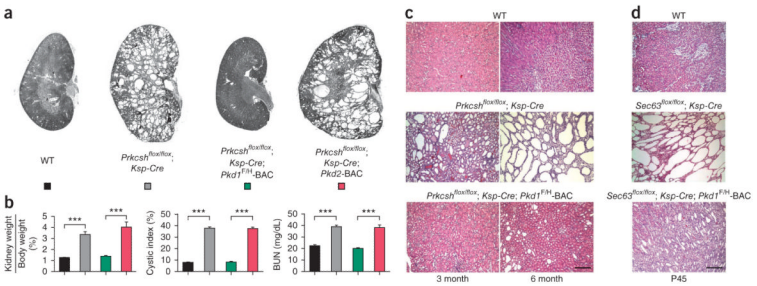


**Figure 4.**

Late stage tubule dilation in *Prkcsh* and *Sec63* mutant kidneys overexpressing PC1 (**a,b**). Histological kidney sections (**a**) and aggregate data (*b*) from mice with the indicated genotypes at 3 months of age. Rescue by the *Pkd1*$^{F/H}$-BAC remains complete through 3 months; *Pkd2*-BAC has no effect. *n* (from left to right) = 6, 7, 7, 5. Results are mean ± s.e.m. (ANOVA; ***P < 0.001). (**c**) Histological examination of *Prkcsh* mutant kidneys with the indicated genotypes at 3 and 6 months. The occurrence of microscopic tubule dilation at 6 months in *Prkcsh*$^{flox/flox}$; *Ksp-Cre*; *Pkd1*$^{F/H}$-BAC kidneys shows that PC1-dependent cyst growth is a function of both gene dosage and time. (**d**) Mild onset cystic dilation in *Sec63*$^{flox/flox}$; *Ksp-Cre*; *Pkd1*$^{F/H}$-BAC at P45 (bottom panel) indicate similar temporal effects in *Sec63* mutants. Scale bars, 500 μm.

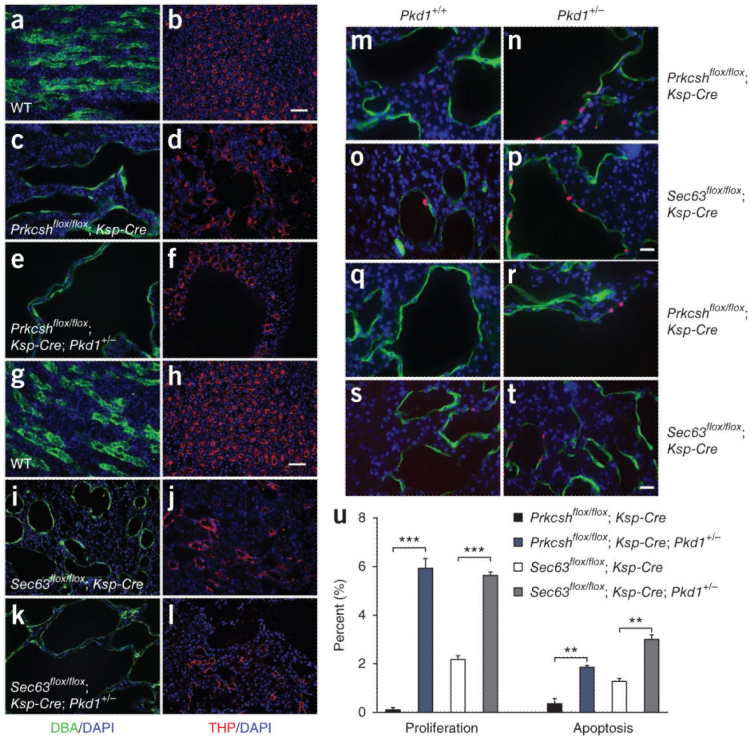


**Figure 5.**

Nephron segment-specific sensitivity to *Pkd1* dosage-dependent proliferation and cyst growth. (**a–l**) Immunocytochemical analysis of *Prkcsh* mutant kidneys at P42 (**a–f**) and *Sec63* mutant kidneys at P21 (**g–l**) showing the increased size of collecting duct cysts (green) resulting from the **Pkd1**$^{+/-}$ background (**c,e,i,k**). Thick ascending limb cysts (red) are unchanged by reduced dosage of *Pkd1* (**d,f,j,l**). DBA, dolichos biflorus agglutinin; THP, Tamm Horsfall protein. Scale bars, 50 μm. (**m–p**) Representative images showing nuclear BrdU incorporation following five daily injections ending at P42 (**m,n**) or a single injection 3 h before being killed on P21 (**o,p**) to determine the impact on cyst proliferation of two copies of *Pkd1* (**m,o**) compared to a single copy (**n,p**). We determined the comparative proliferation rates by counting >1,000 DBA-positive cystic collecting duct cells per kidney from six kidneys for each genotype. BrdU-positive nuclei are shown in red, DBA is green and DAPI is blue. Scale bar, 20 μm. For both ADPLD models, the increased growth of collecting duct cysts with reduced PC1 dosage on the *Pkd1*$^{+/-}$ background was associated with increased proliferation (**u**) (***P < 0.001; mean ± s.e.m.; Student's *t*-test). (**q–t**) Representative images comparing apoptotic rates by TUNEL staining (red) for both ADPLD models as a function of *Pkd1* dosage. (**u**) Apoptotic rates measured as above showed more modest increases on the *Pkd1*$^{+/-}$ background (**u**) (**P < 0.01; mean ± s.e.m.; Student's *t*-test), suggesting that the proliferative effects predominate. DBA, green; scale bar, 20 μm.

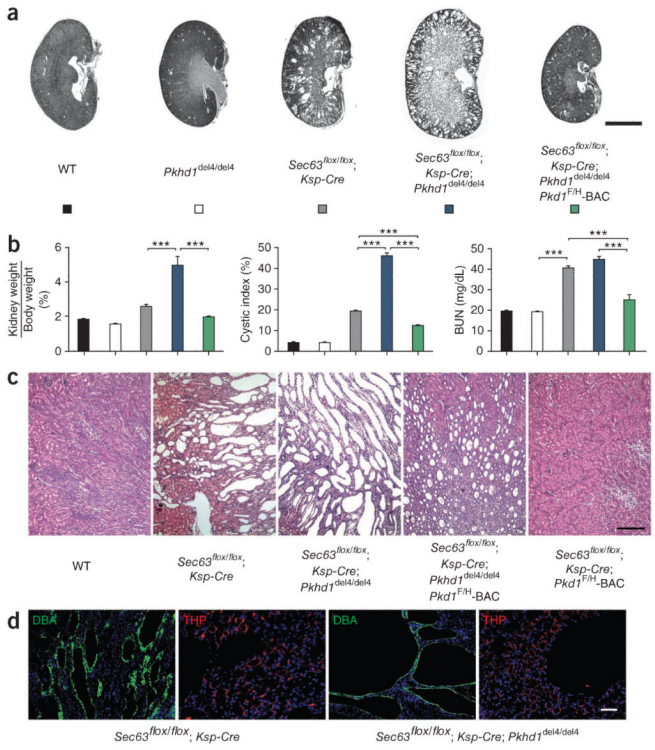


**Figure 6.**

Genetic interaction of *Pkhd1*, *Pkd1* and *Sec63*. (**a–c**) Histological kidney sections (**a,c**) and aggregate structural and functional data (**b**) from mice with the indicated genotypes at P21. The *Pkhd1*$^{del4/del4}$ background results in increased severity of polycystic disease in *Sec63* mutant kidneys. PC1 overexpression rescues the worsened *Sec63*$^{flox/flox}$; *Ksp-Cre*; *Pkhd1*$^{del4/del4}$ phenotype to a level that is milder than *Sec63*$^{flox/flox}$; *Ksp-Cre* alone (**a–c**), although microscopic cysts persist (**c**). Genotypes in the histograms (**b**) are indicated by the colors in **a**; *n* (from left to right) = 5, 6, 8, 6, 6. Results are mean ± s.e.m.; ANOVA; ***P < 0.001. (**d**) Immunocytochemical analysis of *Sec63* mutant kidneys at P21 showing the increased size of collecting duct cysts (green) resulting from the *Pkhd*$^{del4/del4}$ background. Thick ascending limb cysts (red) are unchanged. Scale bars, 2 mm (**a**); 500 μm (**c**); 50 μm (**d**).

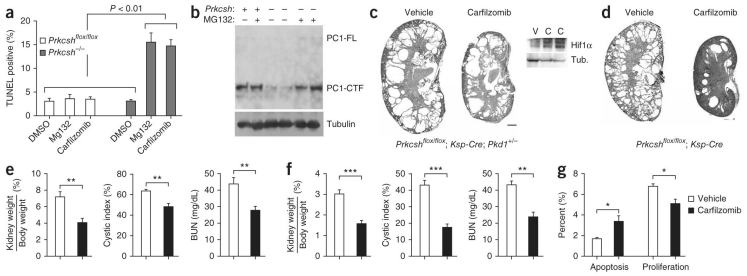


**Figure 7.**

Proteasome inhibitor therapy ameliorates cyst formation following loss of *Prkcsh*. (**a**) *Prkcsh*$^{-/-}$ cells have increased sensitivity to proteasome inhibitors ($n = 3$ independent wells for each genotype and treatment). Results are shown as mean ± s.e.m. (Student's *t*-test). (**b**) *Prkcsh*$^{-/-}$; *Pkd1*$^{F/H}$-BAC cells treated with MG132 (10 μM for 16 h) showed increased levels of PC1. (**c**) Representative images of kidneys from *Prkcsh*$^{flox/flox}$; *Ksp-Cre*; *Pkd1*$^{+/-}$ mice treated twice weekly with carfilzomib (5 mg/kg) for 3 weeks beginning at P21. Effective inhibition of proteasome function is indicated by increased Hif1 α expression in carfilzomib-treated kidneys (**C**) compared to the vehicle-treated controls (**V**). Scale bar, 1 mm. (**d**) Representative images of kidneys from *Prkcsh*$^{flox/flox}$; *Ksp-Cre* mice treated with carfilzomib (5 mg/kg) for 6 weeks beginning at P42. (**e**) Aggregate data for *Prkcsh*$^{flox/flox}$; *Ksp-Cre*; *Pkd1*$^{+/-}$ mice showing improvement following carfilzomib treatment ($n = 6$, carfilzomib group; $n = 5$, vehicle group; results are mean ± s.e.m.; Student's *t*-test; $^{**}P = 0.0011$ (weight ratios), $P = 0.0082$ (cystic index), $^{**}P = 0.0084$ (BUN)). (**f**) Aggregate data for *Prkcsh*$^{flox/flox}$; *Ksp-Cre* mice showing improvement in the carfilzomib-treated group ($n = 6$, carfilzomib group; $n = 3$, vehicle group; results are mean ± s.e.m.; Student's *t*-test; $^{***}P = 0.0007$ (weight ratios), $P < 0.0001$ (cystic index), $P = 0.0032$ (BUN)). (**g**) The rate of apoptosis is increased ($^{*}P = 0.034$), and the rate of proliferation decreased ($^{*}P = 0.025$) in cyst-lining epithelia following treatment with carfilzomib in *Prkcsh*$^{flox/flox}$; *Ksp-Cre*; *Pkd1*$^{+/-}$ mice at P42. Results are mean ± s.e.m. (Student's *t*-test).